ELSEVIER

Catalysis Today 50 (1999) 261–270

CATALYSIS TODAY

Preparation of zirconia–ceria materials by soft chemistry

S. Rossignol, Y. Madier, D. Duprez*

Laboratoire de Catalyse en Chimie Organique, UMR 6503, Faculté des Sciences, 40 Avenue du Recteur Pineau, 86022, Poitiers Cedex, France

Abstract

New zirconia–ceria materials were prepared by soft chemistry with thermal treatments at temperatures below 1000°C. Samples were characterized by XRD, DTA–TGA, BET area measurements and oxygen storage capacity (OSC) measurements. For the preparation, cerium nitrate and different zirconium precursors were used: zirconyl nitrate or chloride for coprecipitation and zirconium propoxide for the modified sol–gel method. Both the structure and the texture of those solids depend on the synthesis and the zirconium precursor. For solids prepared by the modified sol–gel method, with a surface area of 60 $m^2\ g^{-1}$, a new cubic phase ($Zr_{0.25}Ce_{0.75}O_2$) is obtained, while an orthorhombic zirconia phase was identified for solids prepared either by coprecipitation or sol–gel methods. The sol–gel method was particularly efficient for preparation of Ce–Zr–O mixed oxides with high cerium contents. OSC values were significantly higher than in the case of coprecipitated oxides.

Keywords: Zirconia–ceria; Soft chemistry; Coprecipitation; Sol–gel method

1. Introduction

Many studies have been reported concerning the preparation of zirconia–ceria solid solutions for the application in various domains: ceramic powders, catalysis, etc. [1–3]. Based on their excellent thermal stability and their high OSC, use of zirconia–ceria mixed oxides as component of three way catalysts for treatment of automotive exhaust gas represents a great deal [4,5]. The structure stability and the high OSC have been demonstrated for zirconia-doped ceria of cubic structure over a wide range of ceria concentration [6]. These materials are generally prepared either at low temperature by the coprecipitation of the corresponding salts, or at high temperature by firing both oxides [1,4,5,7–9]. Depending on the Ce/Zr ratio and the calcination temperature, three different structures (monoclinic, tetragonal or cubic) are observed for the ZrO_2–CeO_2 system [4,7,9,10].

The goal of the present study was to prepare zirconia–ceria solid solutions ($Zr_{1-x}Ce_xO_2$ with $0 \leq x \leq 1$) by two different methods: conventional ''coprecipitation'' and ''modified sol–gel'' preparation. The influence of the composition and the nature of the precursor on the structure, the texture and the OSC of the samples is discussed.

2. Experimental procedures

2.1. Synthesis

In what follows, the solution volumes and their concentrations are given for the preparation of a 3 g sample. All reactants and solvents were 99% purity

*Corresponding author. E-mail: daniel.duprez@hermes.campus.univ-poitiers.fr

0920-5861/99/$ – see front matter
PII: S0920-5861(98)00508-2

Aldrich products. They were used as delivered, without any further purification.

- *Modified sol–gel method*. The precursor used in this case was the zirconium *n*-propoxide ($Zr(OC_3H_7)_4$) dissolved in 20 ml of isopropyl alcohol. The addition of an aqueous solution of $Ce(NO_3)_3{\cdot}6H_2O$ (20 ml) to the zirconium alkoxide solution immediately leads to the hydrolysis of the mixture and the formation of a pseudo-gel.
- *Coprecipitation method*. Two zirconium precursors were used: $ZrOM_2{\cdot}8H_2O$, $M = NO_3^-$ or Cl^-. A hydrous zirconia–ceria solid solution is obtained by coprecipitation with 12 ml of NH_4OH (14.7 M) of a mixture of $Ce(NO_3)_3{\cdot}6H_2O$ (20 ml in distilled water) and $ZrOM_2$ (20 ml in distilled water). The hydrous precipitate is filtered, redispersed in 100 ml of NH_4OH (0.25 M) for $M = NO_3^-$ or in 100 ml of acetone for $M{=}Cl^-$ and filtered again. In the case of $M{=}Cl^-$, the precipitate is washed until no more chloride ions are detected in the filtrate (test with $AgNO_3$).
- *Pure oxides*. For the preparation of ZrO_2, the same procedure is used by replacing the cerium nitrate solution by distilled water (20 ml). Two CeO_2 samples were prepared by precipitation of an aqueous solution of $Ce(NO_3)_3{\cdot}6H_2O$ with ammonia. The first sample was washed with 100 ml of NH_4OH (0.25 M) and the second one with 100 ml of acetone.

All washed precipitates and pseudo-gels were dried at 60°C for 1 h and then at 120°C overnight. The dried powders were finally calcined in air at 600°C for 4 h.

A classification of the samples by precursor and cerium content is given in Table 1.

2.2. Characterization techniques

Differential thermal analysis (DTA) was used to characterize the solids dried at 120°C. DTA experiments are carried out in dry air between 25°C and 500°C (linear ramp rate of 5°C min^{-1}) by using a Thermal Analyst 2100 Instrument. In fact, preliminary experiments showed that no DTA peak is observed above 500°C.

Specific surface areas were determined by N_2 adsorption at −196°C (one point Brunauer–Emmett–Teller (BET) method) using a Micromeritics Flow Sorb II.

XRD analyses of powders calcined at 600°C were carried out on a Siemens D500 powder diffractometer using Cu K_α radiation (1.5406 Å). Crystalline phases were identified by comparison with the ICDD file (ZrO_2: 37-64 (monoclinic), 37-1413 (orthorhombic), 17-0923 and 42-1164 (tetragonal); $Zr_{0.84}Ce_{0.16}O_2$: 38-1437 (tetragonal); $Zr_{0.25}Ce_{0.75}O_2$: 28-271 (cubic); CeO_2: 34-394 (cubic)). Diffraction peaks fitting is obtained with Profile, a Socabim program, using a splitted pseudo-voigt model for peak profile.

OSC was measured at 400°C in flowing He (1.8 l h^{-1}) on a 20 mg sample. Alternate pulses (0.28 cm^3) of O_2 and CO were used to simulate lean and rich conditions in an engine. Oxygen storage can be evaluated from CO consumption or CO_2 formation (CO pulses) or from O_2 consumption (O_2 pulses). Whatever the method employed, very close OSC values are obtained.

Table 1
Samples prepared via the modified sol–gel method (Zr propoxide) or by coprecipitation (zirconyl nitrate or zirconyl chloride)

Ce (mol%)	Precursors		
	$Ce(NO_3)_3{\cdot}6H_2O$ $Zr(OC_3H_7)_4$	$Ce(NO_3)_3{\cdot}6H_2O$ $ZrO(NO_3)_2$	$Ce(NO_3)_3{\cdot}6H_2O$ $ZrOCl_2{\cdot}8H_2O$
0	A1	A2	A3
16	B1	B2	B3
50	C1	C2	C3
60	D1	D2	D3
75	E1	E2	E3
90	G1	G2	G3
98	H1	H2	H3
100	–	I2	I3

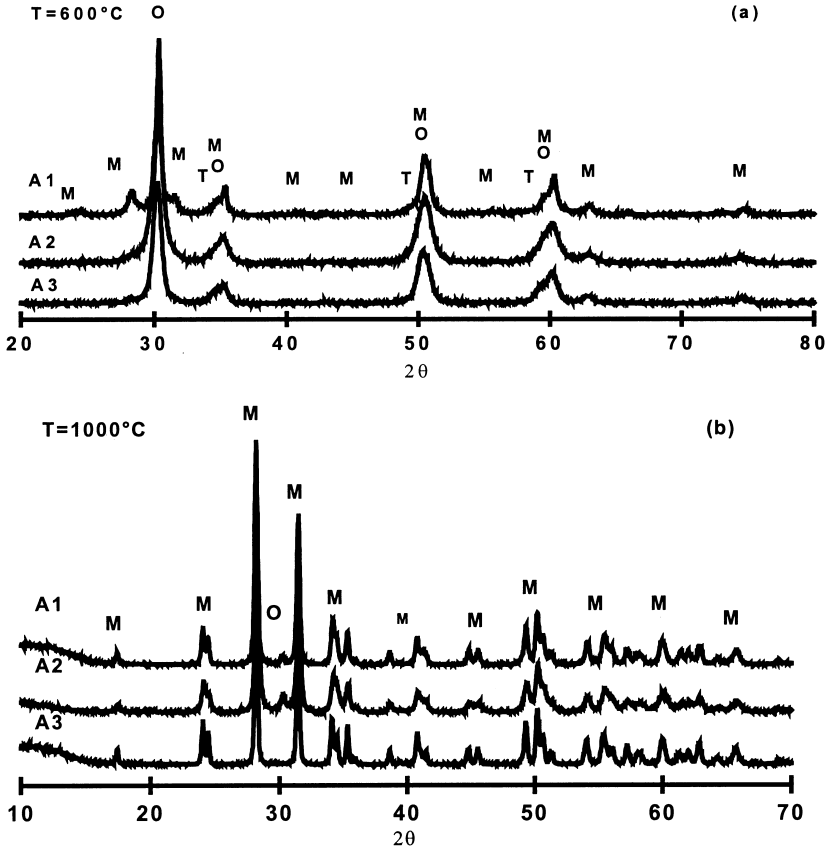

Fig. 1. XRD patterns of ZrO_2 samples prepared from Zr propoxide (A1), zirconyl nitrate (A2) or zirconyl chloride (A3) and calcined at 600°C **(a)** or 1000°C **(b)**. ICDD file: (M) ZrO_2 monoclinic: 37-64, (T) ZrO_2 tetragonal: 42-1164, (O) ZrO_2 orthorhombic: 37-1413.

3. Results and discussion

3.1. Pure oxides

3.1.1. ZrO_2

Whatever the zirconium precursor is, a mixture of crystalline phases is obtained (Fig. 1(a)). The baddeleyite monoclinic structure is not pure but mixed with an orthorhombic phase, which is predominant after calcination at 600°C. For sample A1 we also observe a minor tetragonal phase. Only sample A3, after calcination at 1000°C, is constituted of a pure monoclinic phase (Fig. 1(a′)).

Monoclinic and tetragonal structures are the most common crystalline forms of zirconia. The orthorhombic structure is rarely found. Suyana et al. [11] showed that the orthorhombic phase can be formed above 300°C. We were able to synthesize this orthorhombic phase at temperatures below 1000°C.

In DTA thermograms an exothermic peak at about 420°C is likely related to the crystallization of ZrO_2 (Fig. 2). For the A2 sample this peak is shifted to higher temperatures. This may be explained by the presence of small amounts of baddeleyite, which is in agreement with the previous works [12–15].

3.1.2. CeO_2

XRD patterns of CeO_2 (I2,I3) correspond to a single phase of fluorite-type structure [16] (Fig. 3(a)). The formation of this unique phase is related to the presence of an endothermic peak at about 220°C in the DTA thermogram (Fig. 3(b)).

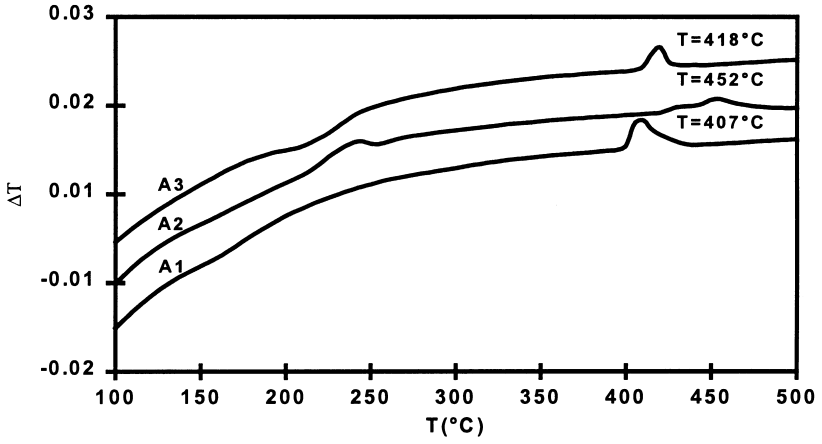

Fig. 2. DTA thermograms of ZrO_2 samples prepared from Zr propoxide (A1), zirconyl nitrate (A2) or zirconyl chloride (A3).

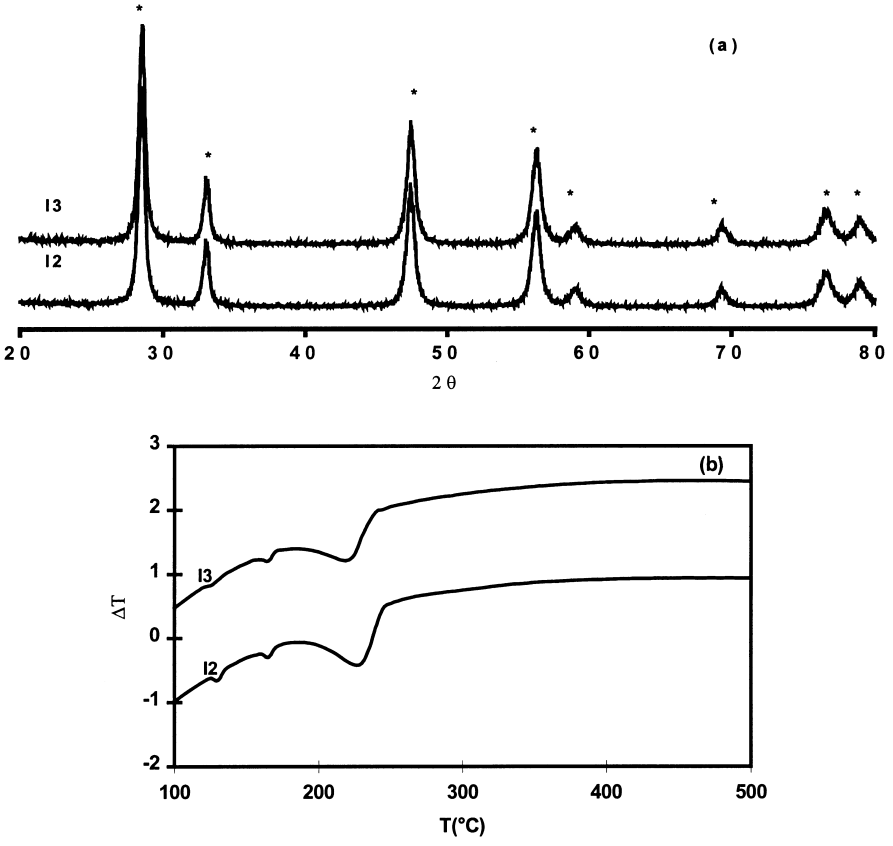

Fig. 3. (a) XRD patterns and (b) DTA thermograms of CeO_2 samples: I2 (washed with NH_4OH) and I3 (washed with acetone) – (∗) CeO_2: 34-114 ICDD file.

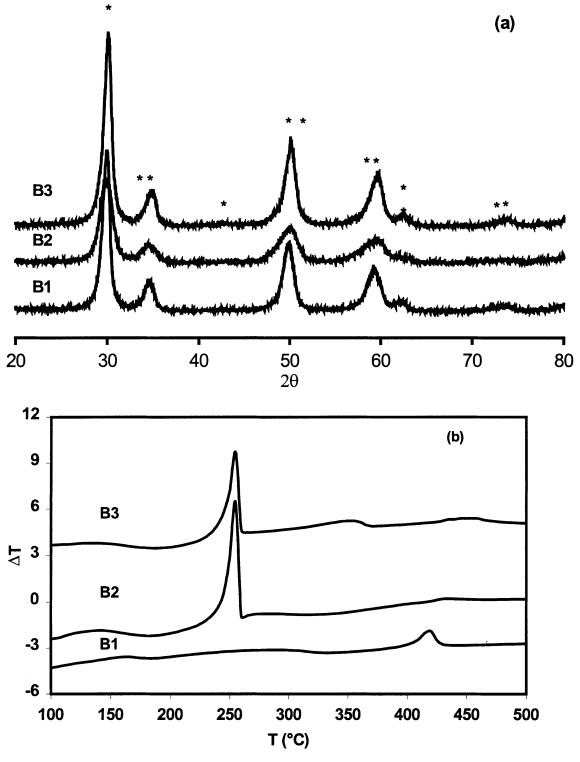

Fig. 4. (a) XRD patterns and (b) DTA thermograms of mixed oxide (x_{Ce}=0.16) prepared with different zirconium precursors – (∗) $Zr_{0.84}Ce_{0.16}O_2$: 38-1437 ICDD file.

3.2. Mixed oxide x_{Ce}=0.16

X-ray patterns of $Zr_{0.84}Ce_{0.16}O_2$ samples, prepared with different zirconium precursors (B1, B2 and B3), are presented in Fig. 4(a). These solids have a tetragonal structure, with nominal composition $Zr_{0.84}Ce_{0.16}O_2$, as observed by Meriani and Spinolo [17]. DTA profiles show a single exothermic peak at about 420°C (Fig. 4(b)). This peak is related to the crystallization process already observed for pure ZrO_2. For B2 and B3, an exothermic event at about 250°C corresponds to the decomposition of nitrate species possibly retained in the solids washed and dried at 120°C. In the presence of a very intense peak at 250°C, the peak at 420°C cannot be seen easily (Fig. 4(b), sample B2 and B3).

3.3. Mixed oxides $x_{Ce}\geq$0.50 (modified sol–gel method)

Fig. 5(a) and (b) show XRD patterns and DTA thermograms of samples C1, D1, E1, G1 and H1. For comparison, data corresponding to sample I2 (pure CeO_2) were added. Whatever the percentage of cerium, a fluorite-type structure is identified. The difference between the lattice parameters of the two fluorite-type structures: a=5.3490 Å for $Zr_{0.25}Ce_{0.75}O_2$ and a=5.4113 Å for CeO_2 [16,18], allows to index the XRD pattern and to distinguish between the two phases. Broadening of the first peak at 2θ=28.5° for samples G1 and H1 is assigned to the presence of a solid solution between CeO_2 and $Zr_{0.25}Ce_{0.75}O_2$. For samples C1 (x=0.50) and D1 (x=0.60), the shoulder at 2θ=30.1° (2θ=30.16° in [19]) is attributed to the presence of a ZrO_2 tetragonal phase. This could also explain the line shift towards larger angles observed in that case.

We can conclude that for x_{Ce}<0.75 the major phase is $Zr_{0.25}Ce_{0.75}O_2$ (cubic) with a minor ZrO_2 tetragonal phase. For x_{Ce}>0.75, the presence of a solid solution of cubic structure is identified [20]. For x_{Ce}=0.75, $Zr_{0.25}Ce_{0.75}O_2$ is the only one observed phase. It was the first time that $Zr_{0.25}Ce_{0.75}O_2$ was obtained at such a low temperature (600°C).

DTA thermograms show an endothermic peak linked with the presence of the main cubic phase. The temperature at the peak maximum, T_p, decreases as the cerium percentage increases. For x_{Ce}>0.75, T_p is close to 220°C, which is about what was obtained for pure CeO_2. For lower cerium contents T_p shifts to 250°C, what can be explained by the presence of $Zr_{0.25}Ce_{0.75}O_2$ identified by XRD. The other two endothermic peaks at 130°C and 200°C are, respectively, attributed to the loss of water and to the decomposition of residual nitrates.

In order to check the stability of the $Zr_{0.25}Ce_{0.75}O_2$ phase, the corresponding samples were calcined at 900°C (Fig. 6(a)). A close look to the 25–37.5 2θ-domain shows that the XRD patterns are unchanged (Fig. 6(b)). Once again, for $x_{Ce}\leq$0.75, the cubic $Zr_{0.25}Ce_{0.75}O_2$ phase is unique while for $x_{Ce}\geq$0.75 the cubic solid solution is the only one observed. This demonstrates that these phases are thermally stable [20].

3.4. Mixed oxides $x_{Ce}\geq$0.50 (precipitation method)

For samples prepared by coprecipitation, identical results are obtained whatever the Zr precursor is (nitrate or chloride). Hereafter, we present only the

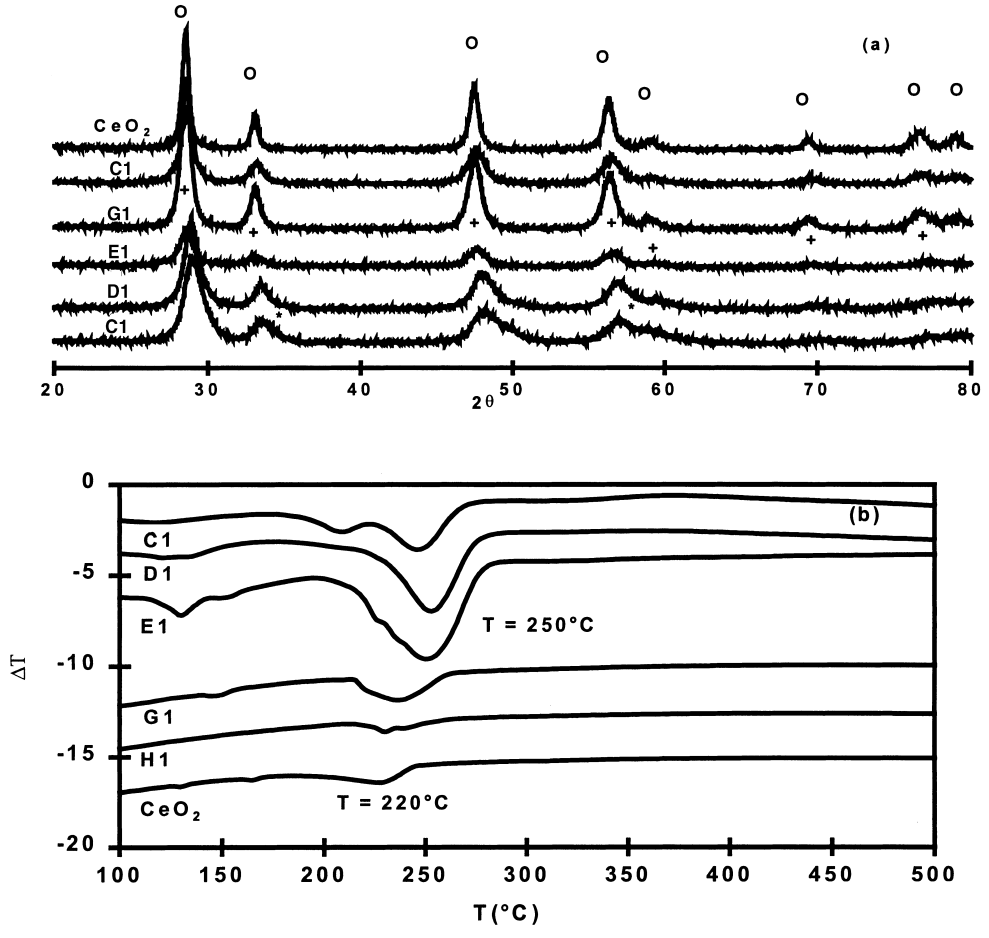

Fig. 5. (a) XRD patterns of samples calcined at 600°C and (b) DTA thermograms of the mixed oxides ($x_{Ce} \geq 0.50$) prepared via the modified sol–gel method using the Zr propoxide – ICDD file: (+) $Zr_{0.25}Ce_{0.75}O_2$: 28-271; (○) CeO_2: 34-394; (∗) ZrO_2: 17-0923.

results obtained for the samples prepared with the zirconyl nitrate precursor (Fig. 7(a) and (b)).

Whatever be the cerium content, a mixture of crystalline phases is observed. The major phase of the fluorite-type structure is ceria. The nature of the minor phase depends on the cerium percentage. For $x_{Ce} \leq 0.90$, the 30.16° 2θ-line is assigned to the tetragonal ZrO_2 [19].

For $x_{Ce} \leq 0.90$, DTA thermograms show an exothermic peak around 240°C corresponding to the decomposition of the residual nitrates. For the other samples, an endothermic peak is observed, attributed to the presence of a CeO_2 phase. The absence of this peak at lower ceria percentage can be explained by the fact that the intensity of the exothermic peak is such that it cancels the endothermic peak. Similarly, the presence of a minor ZrO_2 phase explains the absence of the "crystallization" peak at about 420°C observed in the other DTA thermograms (see Figs. 2 and 4(b)).

3.5. *Comparison with the structural data presented in the literature*

In Table 2, data found in the literature are summarized and compared to our results. Both the preparation method and the pretreatment temperature are considered.

Murota's samples prepared by coprecipitation using the zirconium nitrate precursor and calcined at 900°C are structurally similar to our materials obtained by

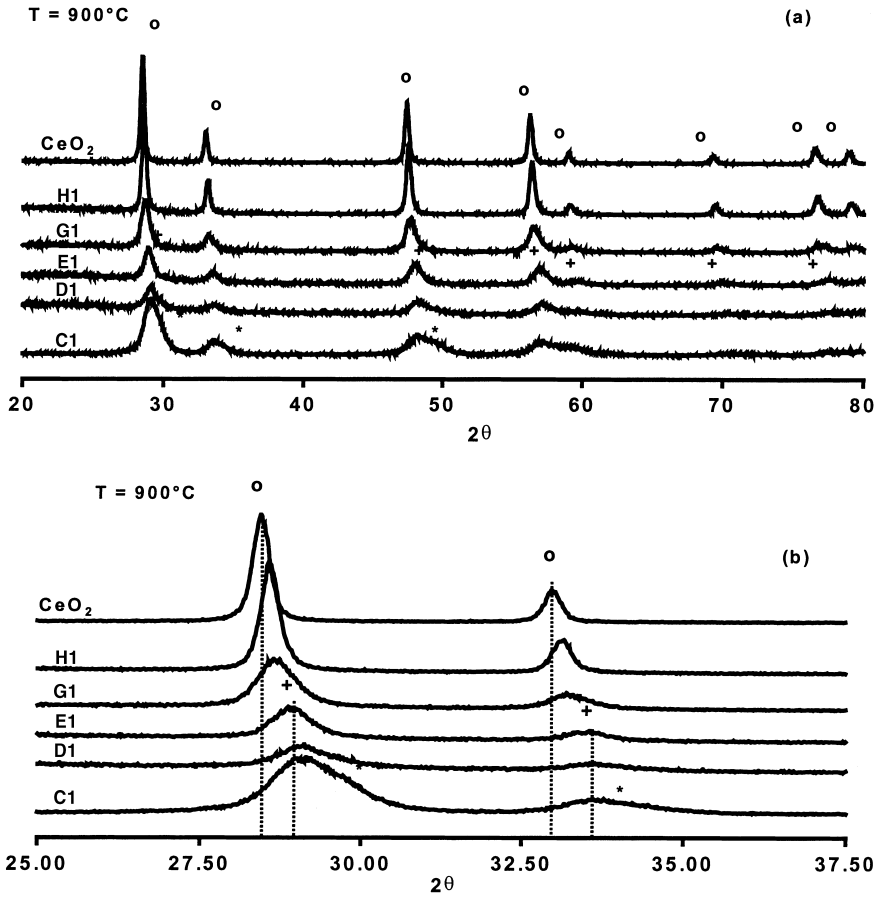

Fig. 6. (a,b) XRD patterns of mixed oxides ($x_{Ce} \geq 0.50$) prepared via the modified sol–gel method and calcined at 900°C. (ICDD file: (+) $Zr_{0.25}Ce_{0.75}O_2$: 28-271; (○) CeO_2: 34-394; (∗) ZrO_2: 17-0923).

coprecipitation with the zirconyl nitrate precursor and calcined at 600°C [5]. Meriani used the sol–gel method to prepare $Zr_{0.50}Ce_{0.50}O_2$ and showed the presence of a mixture of phase [21]. In our case, the structure of $Zr_{1-x}Ce_xO_2$ depends on x. Our most striking result is the formation of a $Zr_{0.25}Ce_{0.75}O_2$ phase even when the preparation conditions should lead to the formation of a phase with a lower stoichiometry in cerium.

If we compare works concerning the preparation of mixed oxides with ceramics preparation methods using pure oxides at high temperatures, sample structures differ from one author to the other [9,10,22–24]. Moreover, results concerning their structure are also different from the results obtained for solids prepared either by sol–gel method or coprecipitation.

These two preparation methods at low temperature allow the synthesis of new materials like $Zr_{0.25}Ce_{0.75}O_2$ obtained by the modified sol–gel method.

3.6. BET area

Results reported in Table 3 show that all the mixed oxides have almost the same specific area. The ceria percentage has no incidence on the specific area. By contrast, the BET area of pure ZrO_2 samples depends on the precursor used for the preparation. The largest surface area is obtained with the zirconyl nitrate precursor. After calcination at 900°C for mixed oxides or 1000°C for pure zirconia, these materials were sintered (Table 2, values in parentheses). The mixed

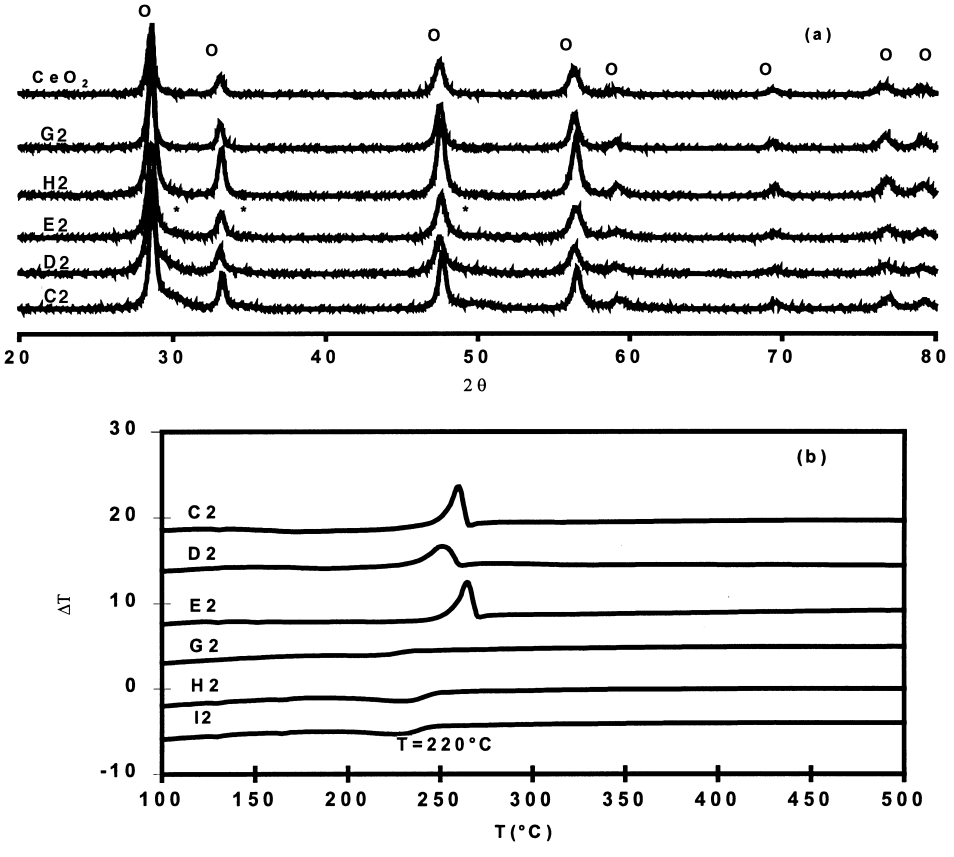

Fig. 7. (a) XRD patterns and (b) DTA thermograms of coprecipitated mixed oxides ($x_{Ce} \geq 0.50$, zirconyl nitrate precursor) calcined at 600°C – ICDD file: (○) CeO_2: 34-394; (∗) ZrO_2: 17–1923.

oxides in any case are much more stable than pure ZrO_2. Among the CeO_2–ZrO_2 samples prepared via the modified sol–gel method, mixed oxides with 75<% Ce<98 show the highest thermal stability.

3.7. Oxygen storage capacity (OSC)

In Fig. 8 are reported as a function of the cerium percentage, the OSC values expressed in μmole of CO consumed per m^2 of the catalyst, measured for the three series of samples calcined at 600°C.

For $x_{Ce} \leq 0.50$, the OSC values are very low. This is in agreement with the tetragonal structure of these materials which is not favorable to oxygen mobility [6,9,26,27].

For $x_{Ce} \geq 0.50$, both propoxide and zirconyl nitrate precursors give better results than the zirconyl chloride precursor. Depending on the precursor, the maximal OSC value is not obtained for the same composition. "Sol–gel" oxides have the highest OSC for $0.75 \leq x \leq 0.98$, while for "coprecipitated" oxides, a plateau is observed above $x=0.50$.

These results demonstrate that the introduction of small amounts of zirconium in the ceria structure induces an exaltation of the oxygen mobility, specially in the case of solids prepared by the modified sol–gel method.

Based on the results presented in Fig. 8, we can also compare the OSC values of materials prepared with the zirconium propoxide precursor and subsequently calcined at 600°C and 900°C.

The higher values obtained at 900°C can be explained by the lower specific area of the samples calcined at 900°C. Whatever the calcination

Table 2
Preparation methods, synthesis conditions and structural characterization of $Zr_{1-x}Ce_xO_2$ solids (M_0: monoclinic ZrO_2; T_0: tetragonal ZrO_2; $T_{0.16}$: tetragonal $Zr_{0.84}Ce_{0.16}O_2$; $C_{0.75}$: cubic $Zr_{0.25}Ce_{0.75}O_2$; C_1: cubic CeO_2; C_x, T_x, M_x: solid solutions and w: weak)

Methods	Precursors	Treatment (°C)	Composition $Zr_{1-x}Ce_xO_2$	Structures[a]	References
Sol–gel	–$Zr(OC_3H_7)_4$; $Ce(NO_3)_3$	600	x=0.16	$T_{0.16}$	Present work
			$0.50 \leq x \leq 0.75$	$C_{0.75}+T_0$(w)	Present work
			x=0.75	$C_{0.75}$	
			$0.75 \leq x \leq 1$	$C_{0.75}+C_1$	
	–$Zr(O\text{-}Bu)_4$; $Ce(acac)_4$	500	x=0.50	$C_{0.50}+T_0$(w)	[7,21,25]
Coprecipitation	–$ZrO(NO_3)_2$; $ZrO(Cl)_2$; $Ce(NO_3)_3$	600	x=0.16	$T_{0.16}$	Present work
			$0.50 \leq x \leq 1$	C_1+T_0	Present work
	–$Zr(NO_3)_4$; $Ce(NO_3)_3$	900	$0.07 \leq x \leq 0.15$	T_x	
			$0.50 \leq x \leq 0.80$	C_x+T_0	[5]
			$x \geq 0.80$	C_x	[5]
Ceramics	–ZrO_2; CeO_2	1400	$0 \leq x \leq 0.20$	M_x	[10,22,23]
			$0.20 \leq x \leq 0.80$	T_x	[10,22,23]
		1590	$x \geq 0.80$	C_x	[10,22,23]
	–ZrO_2; CeO_2		x=0.20	C_x+T_0	[24]
		1600	x=0.50	C_x+T_0	
	–ZrO_2; CeO_2		$0 \leq x \leq 0.20$	M_x	[9]
			$0.20 \leq x \leq 0.50$	C_x+T_0	[9]
			$x \geq 0.50$	C_x	[9]

Table 3
BET surface area of samples calcined at 600°C and higher temperature (numbers in parentheses): 900°C for mixed oxides or 1000°C for pure zirconia

Ce (%)	Specific area ($m^2\ g^{-1}$)		
	$Zr(OC_3H_7)_4$	$ZrO(NO_3)_2$	$ZrOCl_2$
0	21 (5)	87 (6)	36 (2)
16	46 (19)	74	49
50	56 (30)	46	44
60	71 (30)	73	65
75	63 (40)	57	53
90	75 (42)	46	40
98	62 (19)	45	48
100	–	40 (10)	47

temperature is, OSC values remain constant in the 0.75–0.98 Ce% range. In fact these materials preserve the same fluorite-type structure after calcination at 600°C or 900°C. This structure confers to these solids a high oxygen mobility [4,5,26,27].

4. Conclusion

The present work showed that several ZrO_2–CeO_2 systems, with different structures, may be prepared using different zirconium precursors. The specific area of these materials is about 50 $m^2\ g^{-1}$ and does not depend on the mode of the preparation and the ceria percentage.

Preparation of materials by soft chemistry leads to the synthesis of a stable phase at temperatures below 1000°C. The formation of an orthorhombic ZrO_2 phase above 300°C and its transformation into a monoclinic phase at 1000°C was also observed. For $Zr_{1-x}Ce_xO_2$ mixed oxides, only the sol–gel method allows the synthesis of a $Zr_{0.25}Ce_{0.75}O_2$ stable phase.

The $Zr_{0.25}Ce_{0.75}O_2$ phase and solid solutions for Ce-rich mixed oxides appears as good candidates for improving thermal stability and promoting OSC.

Preparation of CeO_2–ZrO_2 mixed oxides by soft chemistry represents a very promising method to obtain stable materials with high oxygen mobility.

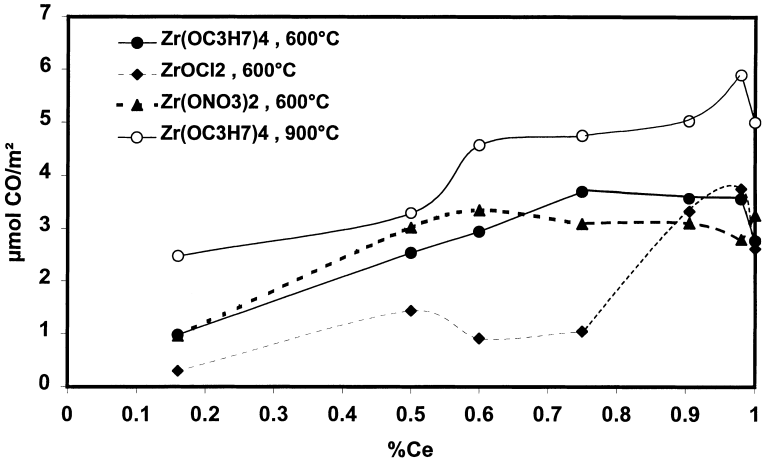

Fig. 8. OSC values (µmol CO m^{-2}), determined at 400°C, of mixed oxides prepared from three different zirconium precursors via the sol–gel method and calcined at 600°C or 900°C.

Acknowledgements

We are grateful to C. Dhenin for her technical help in carrying out most of the experiments which are reported in this paper.

References

[1] T. Sato, K. Dosaka, M. Ishitsuka, E.M. Haga, A. Okuwaki, J. Alloys Compounds 193 (1993) 274.
[2] B. Fegley, A. Barringer, Mater. Res. Soc. Symp. Proc. 32 (1984) 187.
[3] E. Tani, M. Yoshimura, S. Somiya, J. Am. Ceram. Soc. 66(7) (1983) 506.
[4] C. Leitenburg, A. Trovarelli, F. Zamar, S. Maschio, G. Dolcetti, J. Llorca, J. Chem. Soc., Chem. Commun. (1995) 2181.
[5] T. Murota, T. Hasegawa, S. Aozasa, H. Matsui, M. Motoyama, J. Alloys and Compounds 193 (1993) 298.
[6] M. Ozawa, M. Kimura, A. Isogai, J. Alloys and Compounds 193 (1993) 73.
[7] P. Fornasiero, G. Balducci, R. Di Monte, J. Kaspar, V. Sergo, G. Gubitosa, A. Ferrero, M. Graziani, J. Catal. 164 (1995) 173.
[8] Y.T. Moon, H.K. Park, D.K. Kim, C.H. Kim, J. Am. Ceram. Soc. 78(10) (1995) 2225.
[9] P. Fornasiero, R. Di Monte, R. Rango Rao, J. Kaspar, S. Meriani, A. Trovarelli, M. Graziani, J. Catal. 151 (1995) 168.
[10] M. Yashima, H. Arashi, M. Kakihana, M. Yoshimura, J. Am. Ceram. Soc. 77(4) (1994) 1067.
[11] R. Suyama, T. Ashida, S. Kunkihana, J. Am. Ceram. Soc. 68 (1985) C314.
[12] Z. Feng, W.S. Postula, A. Akgerman, R.G. Anthony, Ind. Eng. Chem. Res. 34 (1995) 78.
[13] Y.T. Moon, H.K. Park, D.K. Kim, C.H. Kim, J. Am. Ceram. Soc. 78(10) (1995) 2690.
[14] T.Y. T Seng, C.C. Lin, J.T. Liaw, J. Mater. Sci 22 (1987) 965.
[15] P.D.L. Mercera, J. G Van Ommen, E.B. M Doesburg, A.J. Burggraaf, J.R.H. Ross, Appl. Catal. 57 (1990) 127.
[16] Natl. Bur. Stand. (US) Monogr. 22 (1983) 38.
[17] S. Meriani, G. Spinolo, Powder Diffraction 2(4) (1987) 255.
[18] JCPDS file 28-271; Smith, McCarthy, Penn State University, ICCD Grant-in Aid, 1975.
[19] JCPDS file 42-1164; US Bureau of Mines, Open File Report.
[20] S. Rossignol, D. Duprez, submitted for publication.
[21] S. Meriani, G. Soraru, in: P. Vicenzini (Ed.), Ceramics Powders, 1983, p. 547.
[22] M. Yashima, K. Morimoto, N. Nobuo, M. Yoshimura, J. Am. Ceram. Soc. 76(7) (1993) 1745.
[23] M. Yashima, K. Morimoto, N. Ishizawa, M. Yoshimura, J. Am. Ceram. Soc. 76(11) (1993) 2865.
[24] M. Yashima, K. Ohtake, M. Kakihana, M. Yoshimura, J. Am. Ceram. Soc. 77(10) (1994) 2773.
[25] G. Balducci, P. Fornasiero, R. Di Monte, J. Kaspar, S. Meriani, G. Graziani, Catal. Lett. 33 (1995) 193.
[26] J.P. Cuif, G. Blanchard, O. Touret, M. Marizi, E. Quéméré, SAE Technical Paper [961906].
[27] K. Yamada, H. Tanaka, M. Yamamato, SAE Technical Paper [970464].